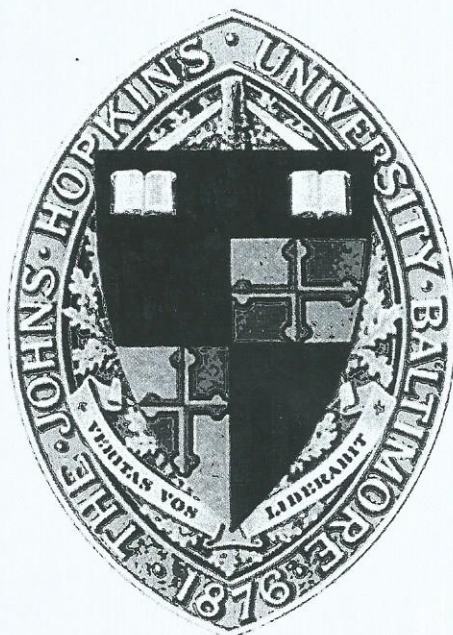


NCdl Nanoclay Research: The Field of Montmorillonite

Past, Present and Future



Ru Chih C. Huang PhD.
Professor of Biology
Johns Hopkins University
2011

The Field of Montmorillonite

Past, Present and Future

I. General Description of Montmorillonite (Nanoclay)

Montmorillonite is a very soft phyllosilicate group of minerals that typically form in microscopic crystals, forming a clay. It is named after Montmorillon in France. Montmorillonite, a member of the smectite family, is a 2:1 clay, meaning that it has 2 tetrahedral sheets sandwiching a central octahedral sheet. The particles are plate-shaped with an average diameter of approximately one micrometre. Members of this group include saponite.

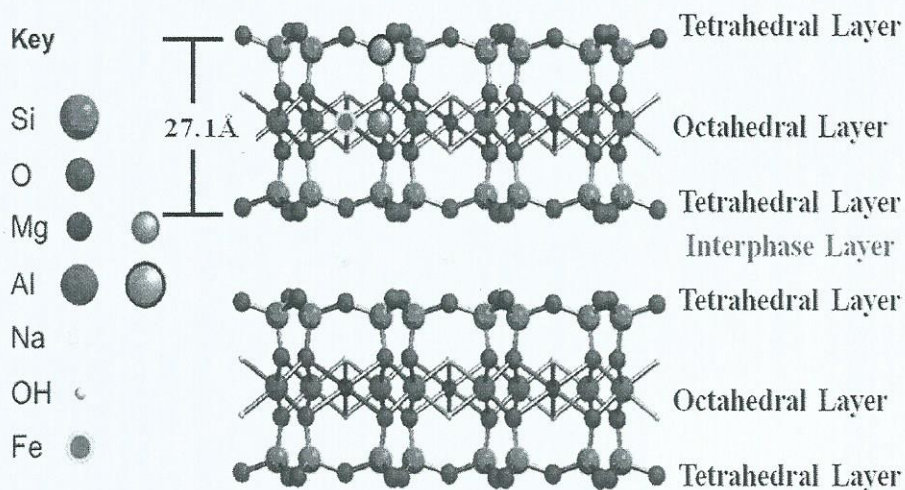
It is the main constituent of the volcanic ash weathering product, bentonite.

The water content of montmorillonite is variable and it increases greatly in volume when it absorbs water. Chemically it is hydrated sodium calcium aluminium magnesium silicate hydroxide $(\text{Na,Ca})_{0.33}(\text{Al,Mg})_2(\text{Si}_4\text{O}_{10})(\text{OH})_2 \cdot n\text{H}_2\text{O}$. Potassium, iron, and other cations are common substitutes, the exact ratio of cations varies with source. It often occurs intermixed with chlorite, muscovite, illite, cookeite, and kaolinite.

Ref.

1. <http://en.wikipedia.org/wiki/Montmorillonite> Last modified on Dec. 14, 2010
2. Purification and properties of *Montmorillonite* *American Mineralogy*; 38, 707-724 (1953).

II. Unit Cell of Montmorillonite



Unit cell of montmorillonite based upon Grim.

Ref. Grim, R. E. *Clay Mineralogy* Seconded (1968)

Ref. Joshi P. C., Aldersley, M. F., Delano J.W. and Ferris J. P. *J. AM. CHEM. SOC.* (2009) 131, 13369-13374.

III. Key References from the Leaders in the Field

a. On Mechanisms of Montmorillonite Catalysis in the Formation of RNA Oligomers

Ref. *J. AM. CHEM. SOC.* (2009) 131, 13369-13374.

Studies from James P. Ferris's group at New York Center for Astrobiology and Rensselaer

b. (1) On montmorillonite accelerating the spontaneous conversion of fatty acid micelles into vesicles clay particles after encapsulated in these membrane vesicles. In addition, RNA adsorbed to clay can be encapsulated within vesicles once formed, such vesicles can grow by incorporating fatty acids supplied as the micelles.

Ref. *Science* (2003) 302, 618-622.

(2) Physical Effects Underlying the Transition from Primitive to Modern Cell Membranes

From single-chain lipids of ancient cell to diacyl or dialkyl glycerol phospholipids of all modern cell membranes

Ref. *PNAS*, Mar. 29, 2011 Vol. 108 5249-5254.

The study was carried out by Jack W. Szostak, a Nobel winner at Howard Hughes Medical Institute, Mass. General Hospital Boston. The paper was reviewed by Gerald F. Joyce, member of the National Academy U.S.A.

IV. A. Progress Report on NC_{dl}: A Descriptive Summary

Structural analysis and anti-HIV activities of NC_{dl} (clay-based PLSNs, polymer layer silicate nanocomposites)

Samples:

Three different preparations of NC_{dl} have been supplied by David C. K. Lo; Managing Director Telekal Co., LTD

Preparations:

- A. Dry white powder (WP app. 30 grams)
- B. 0.8% solution in H₂O, Eyecare prep (EC) app. 50ml
- C. Chopstick (CPS), 4 chopsticks each weighed 10.8g

NC_{dl} Studies and Results

1. The size and chemical composition of a fully water saturated NC_{dl} (EC prep) by dynamic light scattering technology (DLS) and ICPCHEM method respectively.

Jack W. Szostak's group used this technique, for studying the particle size of their NC preparations as described.

(Science: 2003, 302 Supporting Online Material -
www.sciencemag.org/content/302/5645/618/suppl/DC1)

Light scattering and FFF. Dynamic light scattering (DLS) data was collected on a temperature controlled PD2000/Batch instrument (Precision Detectors, Inc. Franklin, MA) at 25°C. Static light scattering (multi-angle laser light scattering, MALLS) particle size measurements were made with a DAWN-EOS instrument, Wyatt Technology Corp. (Santa Barbara, CA), used in flow-mode to analyze the output from a F1000-FO fritoutlet, flow-field fractionation (FFF) system (Postnova Analytics, Salt Lake City, UT). The FFF system was operated with a 30 kD cellulose membrane at a channel flow velocity of 2.0 ml/min and a cross-flow velocity of 0.8 ml/min to optimize the separation of particles in the size range of 50-200 nm. The frit-outlet system was operated at a channel inlet to outlet flow ratio of 2.4 to concentrate the vesicles prior to analysis by the MALLS device.

EC preparation of NC_{dl} was centrifuged at 10,000xg for three minutes at 20°C. The non-pelleted fraction was used for the DLS measurements. Two independent measurements showed the NC_{dl} at 41.8nm (Sample 1) and of 52.24nm (Sample 2) in diameter.

Professor Chia-Chung Chang of NCTU (Email: CCCHANG@Faculty.NCTU.EDU.Tw – Date attached June 17, 2011)

Data attached also included the chemical analysis of the elements of this same NC_{dl} EC preparation.

2. NC_{dl} (white powder preparation) effect on inhibition of HIV-1 replication in infected CD4 positive H₉ cells as determined by using HIV-1 p²⁴ antigen ELSA (*PNAS* 1985, 82: 5199-5262)

Professor Ru Chih Huang and Dr. Ibrahim Adb-Elazem, PhD
Johns Hopkins University and experiments were carried out in P3 laboratory at JHSPH

Data showed NC_{dl} inhibited HIV-1 infection and replication with an IC₉₀ at 40µM.
Data attached

3. Detection of NC_{dl} in HIV-1 infected H₉ cells under the treatment condition as described in section 2 attachment.

Preliminary examination by TEM (procedure attached) was made by Michael McCaffrey, Director Integrated Imaging Center, Johns Hopkins University.

Images of infected NC_{dl} treated H₉ cells were attached. NC_{dl} in various lengths <100nm were detected in HIV-1 infected H₉ cells (attached). A new HIV infection study with NC_{dl} using 10 times more material is currently on-going at JHU/JHSPH. Samples will be ready for the TEM analysis on Aug. 24, 2011.

4. Original sizes of NC_{dl} were examined using Transmission Electron Microscopy (TEM) by J. Michael McCaffrey, Director The Intergrated Imaging Center The Institute for NanoBioTechnology, Johns Hopkins University.

Images of a fully water saturated NC_{dl} showing the length of the nanoparticles in range of 70-300nm were detected. Similarly, the images of NC_{dl} (white powder in ethanol after sonication) showing the length in range of 70-120nm were observed. Imaging pictures are attached.

5. X-ray diffraction (XRD) spectrum of NC_{dl} chopstick preparation (CPS) was made by Dr. H. J. Kao. X-ray diffraction patterns were determined by means of a standard Norel Co unit equipped with Debeye-Scherrer type cameras of radius $180/\pi$ mm. The patterns were produced with FeK α radiation.

Spectrum of a well defined nano-dispersion of NC_{dl} CPS preparation is attached. XRD study of single NC_{dl} crystals remains to be done.

6. Transmission Electron Microscopy (TEM) study of NC_{dl} CPS preparation is currently under investigation both at Dr. Michael McCaffrey's Intergrated Imaging Center at Johns Hopkins University and at Dr. H. J. Kao's laboratory.

Confirmation of NC CPS particle size by TEM will be very important for the structure/function studies of NC_{dl} in the coming months of 2011 and beyond.

B. Progress Report: Supporting Data

Data Attachments

Dear Professor Huang:
Attached please find the results of DLS measurement of nanocracks for your reference.
Regards,
William

Chia-Ching Chang
Professor of Biological Physics
Department of Biological Science and Technology
National Chiao Tung University
Research Fellow
Institute of Physics, Academia Sinica

(1) a.

DLS Report – NanoClaydl

There are two independent measurements for the Nano-Claydl by dynamic light scattering. Both samples have been centrifuged at 10000×g for 3 min.

In first measurement the mean diameter is 41.8 nm Fig 1 and Fig 2, respectively.

Figure 1. DLS measurement of nano-claydl. (a) Correlation function of nano-claydl. The red dots denoted the experiment data and blue curve denoted the NNLS (non-negative least square) fitting of these data. (b) The error of the fitting is approximately 0.32%.

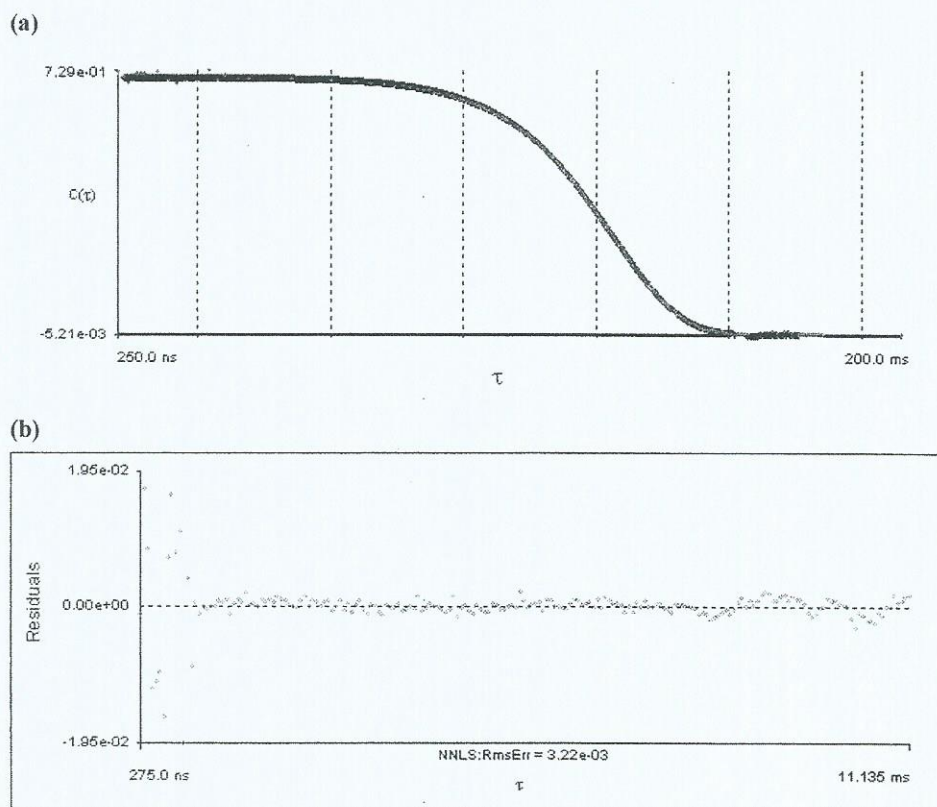
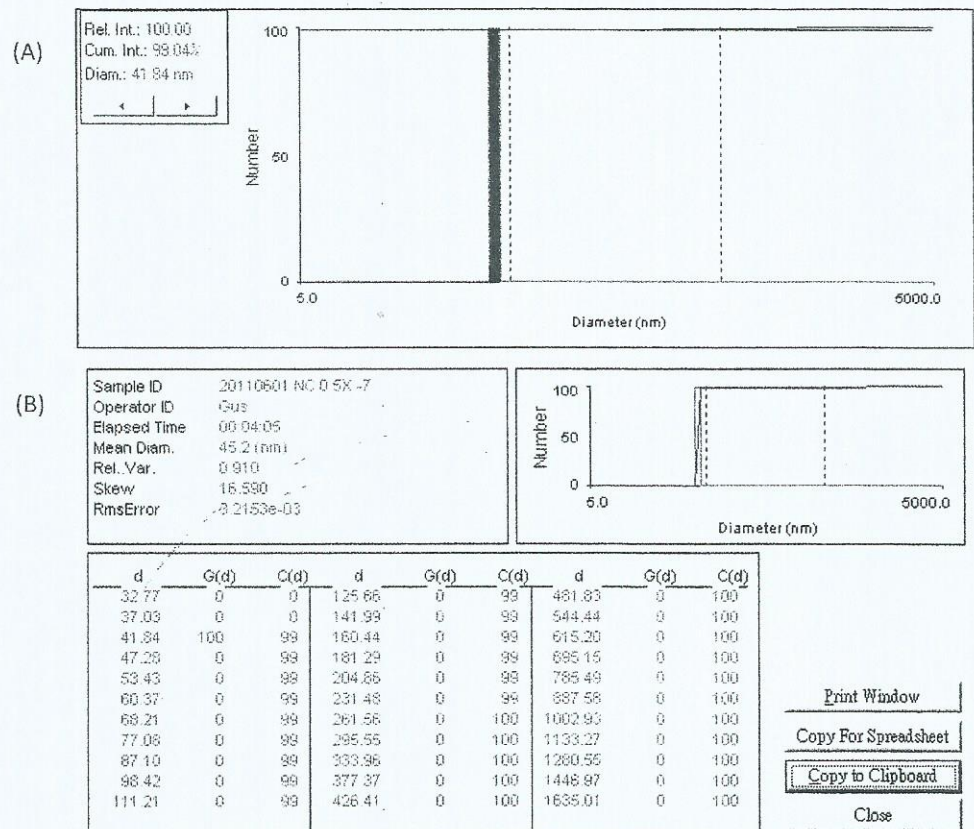
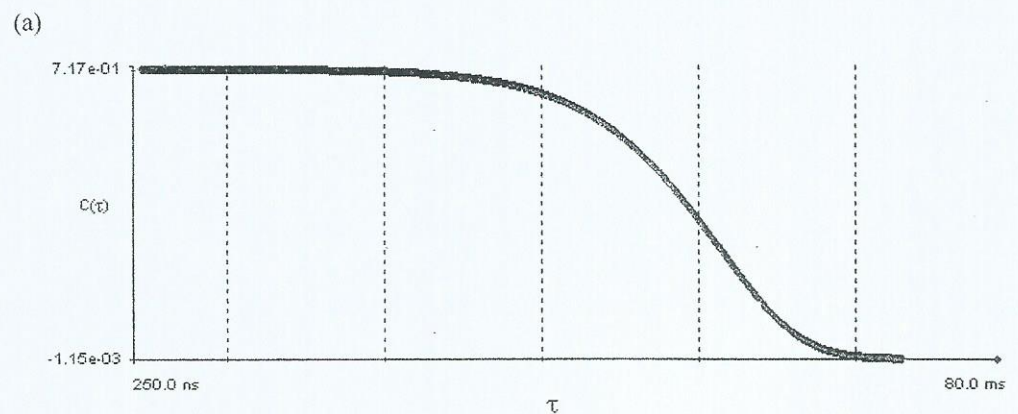


Figure 2. The fitting result of DLS by NNLS (A) The plot is draw by the diameter vs. the relative number of events. (B) The summary of the diameter vs. the relative number in a spreadsheet.



In second measurement the mean diameter is ~52.2 nm in Fig 3 and Fig 4, respectively.

Figure 3. DLS measurement of nano-claydl. (a) Correlation function of nano-claydl. The red dots denoted the experiment data and blue curve denoted the NNLS fitting of these data. (b) The error of the fitting is approximately 0.09%.



(b)

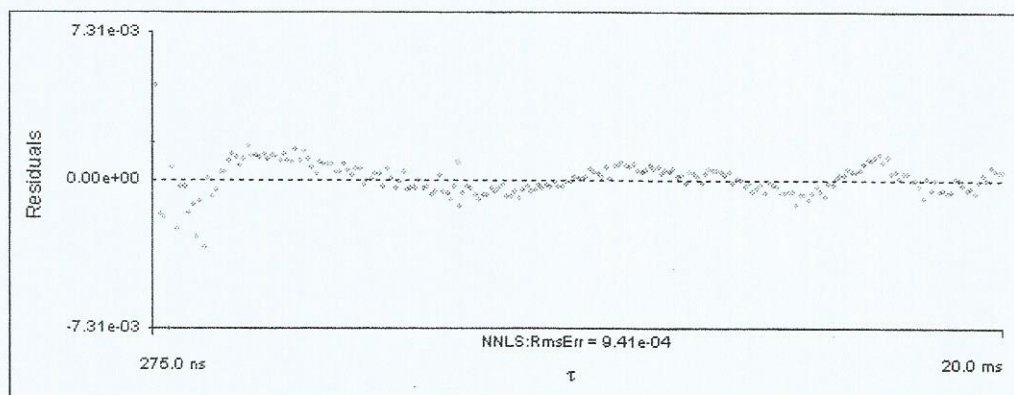
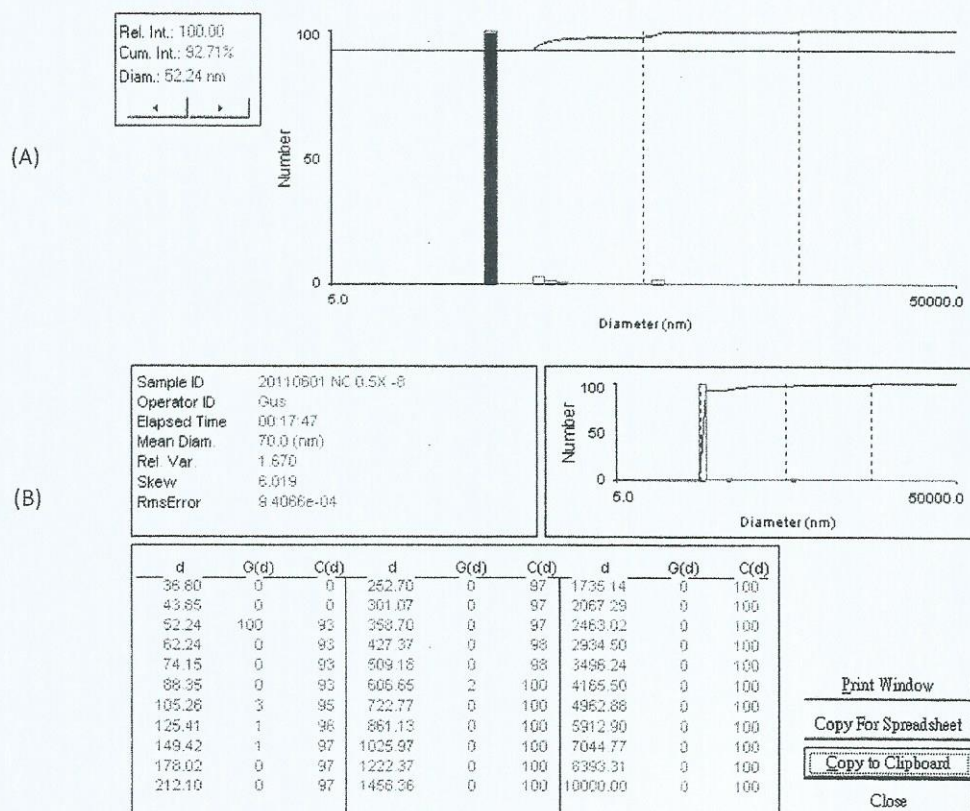


Figure 4. The fitting result of DLS by NNLS (A) The plot is draw by the diameter vs. the relative number of events. (B) The summary of the diameter vs. the relative number in a spreadsheet.



(2) b.

Chemical Composition of NCdl EC Preparation – June 17th

Semi-Quantitation Report - Detailed (Text Only)

File Name : K31.D
 File Path : D:\DATA\FULLSCAN1\
 Method : C:\ICPCHEM\1\METHODS\FULL2_CE.M
 Acq Time : Jun 17 2011 12:01 pm
 Sample Name : Sample
 Sample Type : Sample
 Comments :
 Prep Dilution : 50.00 = (50.00 / 1.000) * 1.000
 Auto Dilution : Undiluted
 Total Dilution : 50.00
 Operator Name: WEN
 Acq Mode : Spectrum
 Bkg File : -----
 Bkg Rejected Masses: -----
 Interference Correction : OFF
 ISTD Correction: OFF
 ISTD File : -----
 ISTD Element 1 : -----
 ISTD Element 2 : -----
 ISTD Element 3 : -----
 ISTD Element 4 : -----
 Blank File : D:\DATA\FULLSCAN1\K30.D
 Tune Step : #1

Eyecare Prep.
0.8% Solution of NCa in
water
Clay-based
PLSNs (Polymer-layered
silicate nanocomposites

	Mass	Conc.	Counts(CPS)	Bkg count	Time(sec)	
Li	7	540.0 ppb	13,667.10	---	0.1	
Be	9	30.00 ppb	550.0333	---	0.1	
B	11	480.0 ppb	6,331.672	---	0.1	
Na	23	260,000 ppb	47,552,540	---	0.1	
Mg	24	120,000 ppb	9,197,382	---	0.1	
Al	27	610,000 ppb	26,750,400	---	0.1	
Si	29	1,600,000 ppb	2,411,904	---	0.1	
P	31	390.0 ppb	1,650.173	---	0.1	
S	34	3,300 ppb	28,260.00	---	0.1	
K	39	9,700 ppb	1,477,289	---	0.1	
Ca	43	7,400 ppb	6,591.819	---	0.1	OXIDE
Sc	45	49.00 ppb	14,358.05	---	0.1	
Ti	47	670.0 ppb	17,282.87	---	0.1	
V	51	30.00 ppb	11,014.97	---	0.1	
Cr	53	-3.900 ppb	760.0511	---	0.1	
Mn	55	190.0 ppb	75,259.07	---	0.1	
Fe	57	140,000 ppb	749,600.8	---	0.1	
Co	59	25.00 ppb	14,648.50	---	0.1	
Ni	60	110.0 ppb	16,700.81	---	0.1	
Cu	63	47.00 ppb	17,091.50	---	0.1	ARGIDE
Zn	66	1,400 ppb	116,714.1	---	0.1	
Ga	69	190.0 ppb	59,131.68	---	0.1	
Ge	72	11.00 ppb	970.0782	---	0.1	
As	75	8.800 ppb	480.0258	---	0.1	
Se	82	18.00 ppb	90.00553	---	0.1	OXIDE
Br	79	9.300 ppb	320.0176	---	0.1	ARGIDE
Rb	85	99.00 ppb	41,416.19	---	0.1	
Sr	88	370.0 ppb	209,279.0	---	0.1	
Y	89	34.00 ppb	33,398.58	---	0.1	
Zr	90	270.0 ppb	150,767.41	---	0.1	

Nb	93	120.0 ppb	127,910.5	---	0.1	
Mo	95	0.7700 ppb	140.0059	---	0.1	
Ru	101	0.2200 ppb	50.00336	---	0.1	OXIDE
Rh	103	<0.04000 ppb	30.00112	---	0.1	
Pd	105	0.5700 ppb	130.0056	---	0.1	OXIDE
Ag	107	0.2800 ppb	160.0067	---	0.1	
Cd	111	1.100 ppb	110.0056	---	0.1	
In	115	0.8500 ppb	890.0735	---	0.1	
Sn	118	120.0 ppb	33,183.95	---	0.1	
Sb	121	1.300 ppb	400.0205	---	0.1	
Te	125	<2.100 ppb	0.0000000	---	0.1	
I	127	3.900 ppb	1,170.112	---	0.1	
Cs	133	81.00 ppb	82,112.07	---	0.1	
Ba	137	310.0 ppb	46,725.91	---	0.1	
La	139	21.00 ppb	37,462.03	---	0.1	
Ce	140	77.00 ppb	128,236.9	---	0.1	
Pr	141	5.900 ppb	13,571.28	---	0.1	
Nd	146	17.00 ppb	7,238.679	---	0.1	
Sm	147	5.200 ppb	1,670.660	---	0.1	
Eu	153	0.3700 ppb	450.0481	---	0.1	OXIDE
Gd	157	6.800 ppb	2,491.920	---	0.1	
Tb	159	0.7300 ppb	1,790.879	---	0.1	
Dy	163	2.800 ppb	1,740.530	---	0.1	
Ho	165	0.8500 ppb	2,090.823	---	0.1	
Er	166	2.900 ppb	2,251.581	---	0.1	
Tm	169	0.5200 ppb	1,320.534	---	0.1	
Yb	172	3.900 ppb	2,481.589	---	0.1	
Lu	175	0.5800 ppb	1,530.796	---	0.1	
Hf	178	18.00 ppb	10,054.78	---	0.1	
Ta	181	29.00 ppb	74,313.05	---	0.1	
W	182	0.7000 ppb	470.0316	---	0.1	HYDRIDE
Re	185	<0.05600 ppb	0.0000000	---	0.1	
Os	189	<-6.600E-6 ppb	10.00039	---	0.1	
Ir	193	0.06500 ppb	80.00394	---	0.1	
Pt	195	<0.09000 ppb	40.00158	---	0.1	
Au	197	0.6000 ppb	450.0263	---	0.1	
Hg	202	<-0.03500 ppb	40.00158	---	0.1	
Tl	205	0.2500 ppb	460.0277	---	0.1	
Pb	208	27.00 ppb	31,131.25	---	0.1	
Bi	209	1.200 ppb	2,060.518	---	0.1	
Th	232	34.00 ppb	78,370.16	---	0.1	
U	238	9.100 ppb	23,216.70	---	0.1	

End of Report

Fri Jun 17 12:06:20 2011

Submitted by Dr. Ming Hwu Tsu, Assistant Researcher NTHU

First Report: NC Effect on HIV-1 Replication in H9 Cells

Preparation of NC in Growth Medium

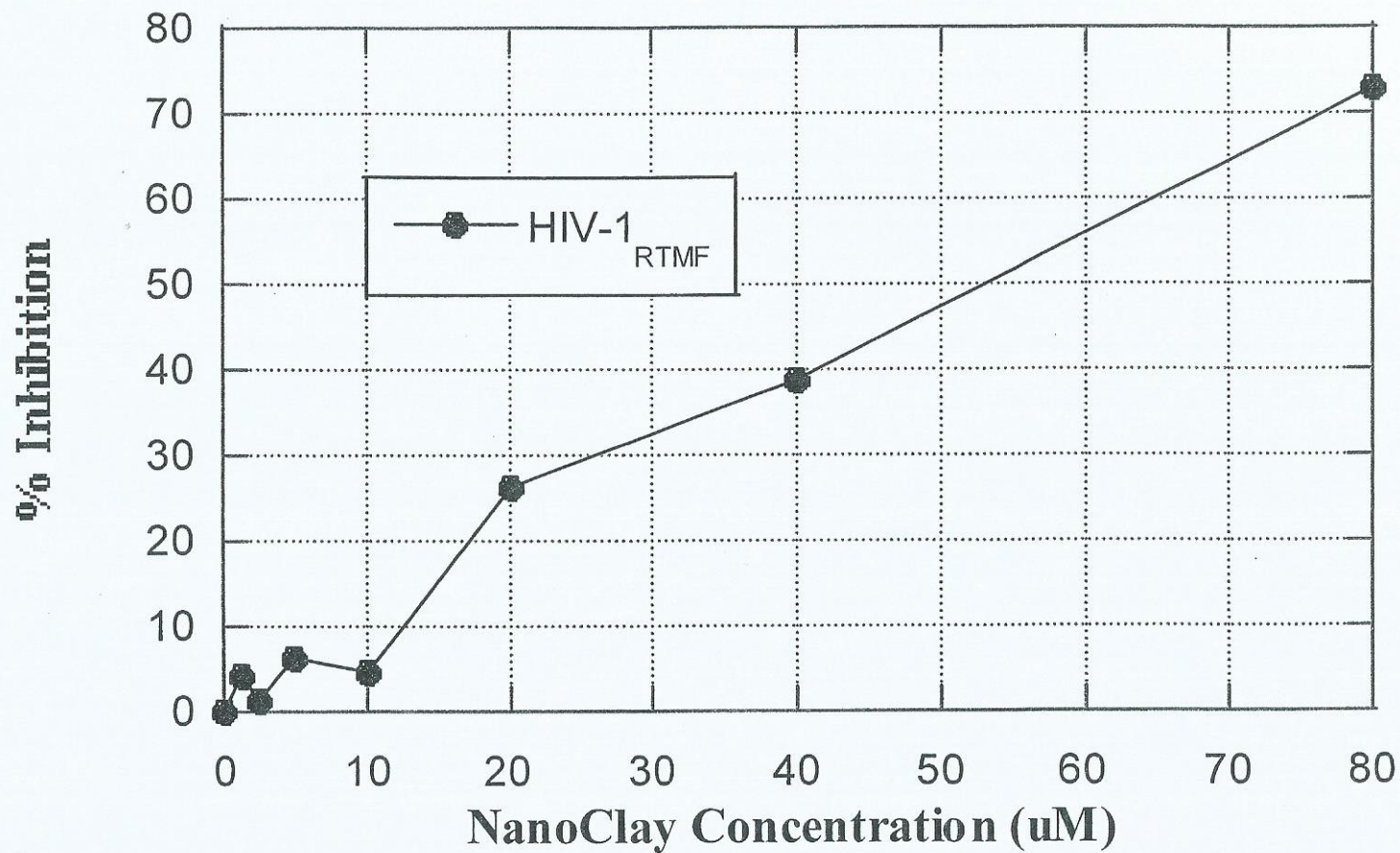
100% RPMI (I)	90% RPMI 10% CPE (II)	NC in 90% RPMI 10% CPE (III)	Final Volume	NC Concentration * (μg)	NC (μM)**
148.8 μl	51.2 μl	0 μl	200 μl	0 $\mu\text{g}/200 \mu\text{l}$	0 μM
148.8 μl	44.8 μl	6.4 μl	200 μl	6.4 $\mu\text{g}/200 \mu\text{l}$	40 μM
148.8 μl	38.4 μl	12.8 μl	200 μl	12.8 $\mu\text{g}/200 \mu\text{l}$	80 μM
148.8 μl	25.6 μl	25.6 μl	200 μl	25.6 $\mu\text{g}/200 \mu\text{l}$	160 μM
148.8 μl	0 μl	51.2 μl	200 μl	51.2 $\mu\text{g}/200 \mu\text{l}$	320 μM

Effect of Nanoclay on HIV-1_{IIIB} Replication in H9 Cells

Concentrations (NanoClay)	Reading of the Replicates Av	Subtration from Average of negative cells (0.057) (No virus and no NanoClay)	Viral % Inhibition
320 μM	0.068 (0.108, 0.049, 0.048)	0.011	99.7
160 μM	0.052 (0.055, 0.05, 0.051)	0.000	100.0
80 μM	0.069 (0.077, 0.062, 0.069)	0.012	99.6
40 μM	0.381 (0.456, 0.451, 0.237)	0.324	90.5
0 μM	3.478 (4.0, 4.0, 2.435)	3.421	---

Rachelle C. Huang

Effect of NanoClay against HIV-1 replication in H9 cells



Rachin C. Huang